

Cumulative Impact Assessment of Tidal Stream Energy Extraction in the Irish Sea

David Haverson^{a,1}, John Bacon^a, Helen C.M. Smith^b, Vengatesan Venugopal^c, Qing Xiao^d

^a Centre for Environment, Fisheries and Aquaculture Science, Lowestoft, NR33 0HT

^b College of Engineering, Mathematics and Physical Sciences, University of Exeter, Falmouth, TR10 9EZ

^c Institute of Energy Systems, University of Edinburgh, Edinburgh, EH9 3DW

^d Department of Naval Architecture, University of Strathclyde, Glasgow, G1 1XQ

Abstract

As the tidal stream industry continues to develop and move towards commercial viability, strategic planning is required to maximise its full potential. A cumulative impact assessment of tidal stream developments in the Irish Sea has been conducted on a high-resolution depth-averaged hydrodynamic model, using Telemac2D. Eight sites were investigated, representing the proposed tidal developments at the time of study. These included: Ramsey Sound (10 MW), Anglesey (10 MW), Strangford Loch (1.2 MW), Mull of Kintyre (3 MW), Torr Head (100 MW), Fair Head (100 MW), Sound of Islay (10 MW) and West of Islay (30 MW). Only three of the eight projects modelled showed array-array interacted: Fair Head, Torr Head and Mull of Kintyre. A smaller domain model, for the three projects was then created for further analysis. Results showed the Mull of Kintyre farm had little overall impact on energy production on Fair Head and Torr Head with itself slightly improving with the presence of the other two projects (+0.09%). Fair Head reduced the energy production at Torr Head by 17%, whereas, Torr Head only reduced energy production at Fair Head by 2%. This was caused by the tidal asymmetry at the site whereby the flood (west to east) was stronger. As Fair Head lies to the west of Torr Head, its impact was greater. Despite both arrays having an installed capacity of 100 MW, the maximum power output during the flood tide is 98.1MW for Fair Head and 64.5 MW for Torr Head, when operating concurrently, representing 31% reduction at Torr Head. If Torr Head can still operate commercially in the presence of Fair Head, then the additional environmental impact of Torr Head, such as the change in bed shear stress, is small. Within the Irish Sea, very few of the tidal projects investigated are geographically within close proximity to each other, meaning their interaction is limited. As the industry grows and the technology matures, allowing sites with lower peak velocities to be exploited, the risk of interaction to these sites will grow when more intermediary sites are developed.

Keywords: Tidal energy, cumulative impact, numerical model, zone of influence

1 Introduction

The development of tidal stream energy extraction technology and the establishment of a tidal stream industry has seen considerable growth in the past two decades [1]. As the tidal stream industry is only just starting to take the first steps moving from testing full-scale prototypes toward commercial viability, strategic planning of the marine environment is needed to maximise its full potential [2]. Many of the high velocity sites suitable for energy extraction are in close proximity and therefore could potentially interact significantly with one another. It is not efficient or in the best interest of the industry to consider each project in isolation. Cumulative impact assessments should be conducted, but have only recently been considered [3,4]. Wilson et al (2012) investigated the interaction between energy extraction from tidal stream and tidal barrages across the UK and its effect on the European continental shelf. Results showed severe near-field effects if tidal stream extraction is not limited and would require close management between nearby projects to limit environmental and economic impacts [4].

Whilst a lot of focus has been given to modelling the Pentland Firth [5-7], it is not the only site being developed within the UK; the Irish Sea also has a number of proposed developments. The Irish Sea has long been studied [8-11]. Depths in the Irish Sea range from intertidal mud flats to ~140m in the central Irish Sea, to the extreme of 250m in the North Channel. Two amphidromic systems are found in the Irish Sea, one on the east coast of Ireland and one to the north of Northern Ireland. Tidal ranges in the east Irish Sea are the largest in the UK, with ranges more than 9m at Workington and 12m at Hinkley [12]. Large tidal velocities (>2m/s) can be found in several locations in the Irish Sea, notably around Pembrokeshire, Anglesey and Northern Ireland [13]. Several studies

¹ Corresponding Author:

E-mail address: david.haverson@cefas.co.uk

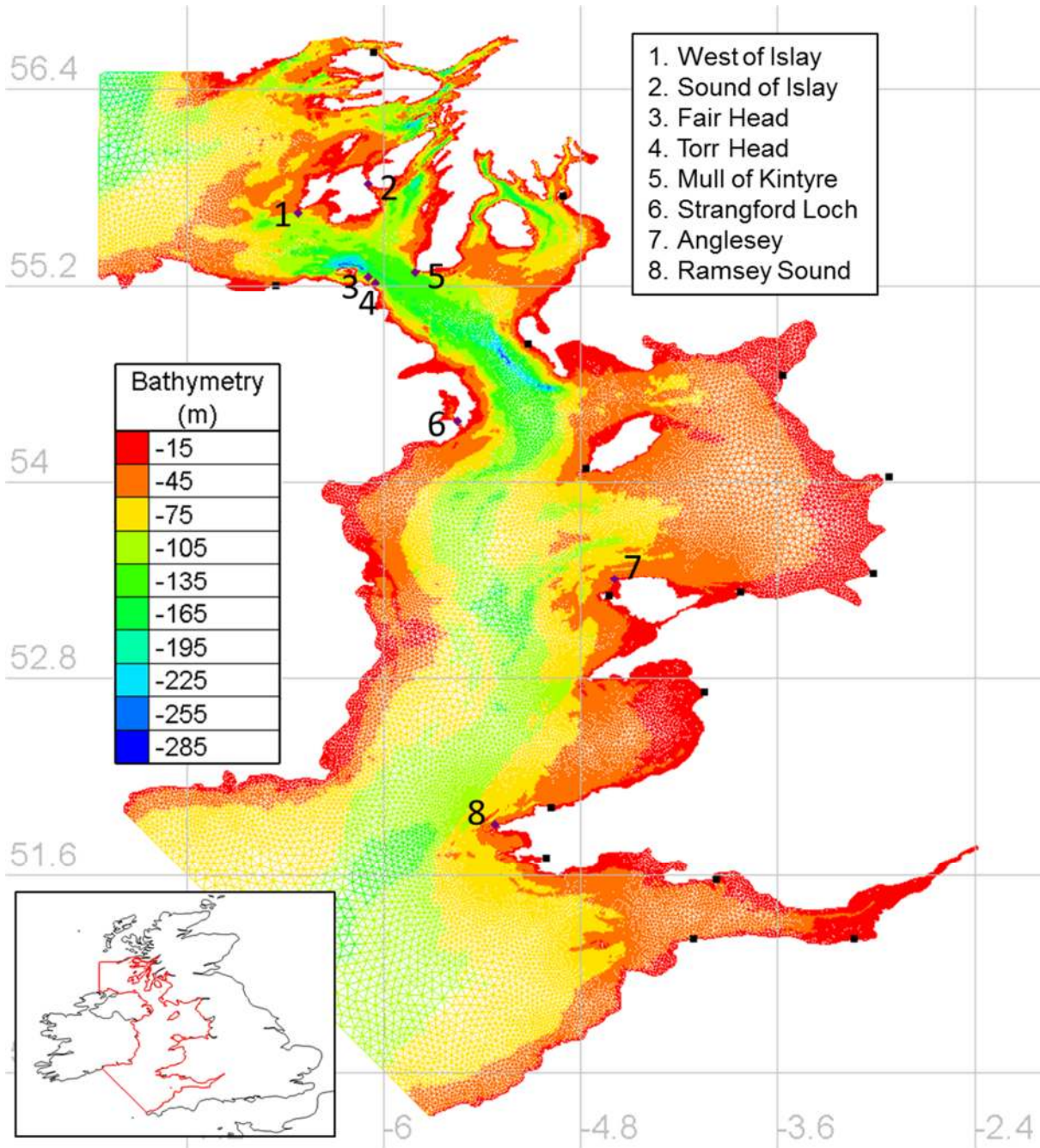
52 have been conducted assessing these locations for the available tidal energy resource and the suitability for tidal
53 stream extraction [13-15]. However, these studies do not include the presence of tidal stream devices, nor the
54 interaction of devices or arrays of devices with one another. Robins et al (2015) investigate how the ratio of the
55 M2 and S2 harmonics can affect the annual practical power and estimate the spatial distribution of a tidal stream
56 capacity factor [13]. Whilst an annual power production is calculated for two sites, the Pentland Firth and
57 Alderney, “*power extraction from individual turbines has not been simulated*” and “*neglect any device*
58 *feedbacks*”. Lewis et al (2015) investigate the total annual mean tidal resource of the Irish Sea within the
59 constraints of 1st generation devices (velocities > 2.5m/s and depths between 25-50m) and show that the total
60 potential resource could be larger if devices could be deployed in water depths greater than 50m [14]. Neil et al.
61 (2014) investigate the phasing of tidal sites around the European shelf for power generation, but conclude there is
62 minimal phase diversity between sites for power generation [15].

63 As well as the discussed resource assessments, studies have been conducted in the Irish Sea including the
64 presence of tidal turbines. Robins et al (2014) assessed the impact of tidal-stream arrays in relation to the natural
65 variability of sedimentary processes at Anglesey, but only included a single tidal array of increasing capacity [16].
66 Hashemi et al. (2015) investigated the influence of waves on tidal resource at Anglesey, showing that extreme
67 wave-current interactions can reduce the tidal resource by 20% [17]. Walkington & Burrows (2009) conducted an
68 assessment of tidal stream power at multiple sites [18]. However, the hydrodynamic effect of the tidal array at
69 each of the four locations was considered in isolation. Furthermore, the tidal turbines were represented as a
70 constant drag term, neglecting the operation of the turbine and the drag due to the support structure, leading to an
71 under-representation of the total force and influence exerted by the turbine.

72 At the time of this study, there were eight existing and proposed tidal projects within the Irish Sea, totalling
73 264 MW. These include: Ramsey Sound (10 MW), Anglesey (10 MW), Strangford Loch (1.2 MW), Mull of
74 Kintyre (3 MW), Torr Head (100 MW), Fair Head (100 MW), Sound of Islay (10 MW) and West of Islay (30
75 MW) (see Figure 1). The size of these arrays represent the actual proposed installed capacities of the site
76 developers and not the maximum theoretical capacities of the sites. Wilson et al (2012) have previously
77 investigated the interaction of extreme future large scale deployments (>85GW by 2050). The aim of this study is
78 to investigate the interaction of actual projects detailed by site developers. Since this work has been undertaken,
79 funding for the Anglesey project was removed and the project stalled. However, for the purpose of this analysis,
80 it has been retained. This paper will investigate the cumulative impact of tidal energy in the Irish Sea to examine
81 the extent to which the projects interact with each other. For this study, only tidal stream developments have been
82 considered; tidal barrages were not included.

83 **2 Irish Sea Model**

84 A high-resolution depth-averaged model of the Irish Sea was built using an unstructured triangular mesh, with
85 the hydrodynamic software Telemac2D (v7p1) [19]. The model domain extends between 50.14°N – 56.72°N and
86 2.38°W – 7.73°W and is shown in Figure 1. The unstructured mesh was discretised with 305,000 nodes, and has
87 a resolution of 15 km around the open boundary, reducing to 1km along the coastline. Bathymetry of the area,
88 relative to Chart Datum, was sourced from the Department for Environment, Food & Rural Affairs UKSeaMap
89 2010 and was provided by the Centre for Environment, Fisheries and Aquaculture Sciences. The resolution of the
90 bathymetry points from this dataset are 1 arc-second (~30m). The bathymetry was corrected to Mean Sea Level
91 by applying the maximum tidal range to the depths. As bathymetry strongly influences hydrodynamic
92 characteristics, a high resolution 2m and 4m resolution bathymetry, from the UK Hydrographic Office (UKHO),
93 has also been applied around Ramsey Sound, Fair Head, Torr Head and the Sound of Islay. The hydrodynamics
94 are forced along the open boundaries using tidal constituents from the OSU TPXO European Shelf 1/30° regional
95 model [20]. As both prescribed elevations and velocities are applied at the boundary, the open boundaries are set
96 far from the area of interest to reduce any dampening on the far field effects of a tidal array. The model uses a k-
97 ε turbulence model. The depth-averaged parameterisation of k-ε in Telemac was developed by Rastogi and Rodi
98 (1978) with the velocity diffusivity set to $1 \times 10^{-6} \text{ m}^2/\text{s}$, representing the kinematic viscosity of water [21]. The
99 Nikuradse law for bottom friction was used, with a constant value of $k_s = 0.04$ applied to the whole model domain.



100

101 **Figure 1: Irish Sea model domain showing the locations of the tidal arrays (purple diamonds) and tide gauge locations**
 102 **(black squares) used for validation.**

103 **3 Modelling tidal turbines**

104 The effect of a tidal array is introduced into the model as an extra sink in the momentum equations. This has
 105 become the common method for modelling tidal turbines [16,22,23]. An individual tidal turbine causes a change
 106 in momentum in two parts: a thrust force produced by the rotor due to energy extraction and a drag force caused
 107 by the supporting structure, i.e.-

108
$$F_D = \frac{1}{2}\rho C_T A_r U^2 + \frac{1}{2}\rho C_D A_s U^2, \quad (1)$$

109 where U is the upstream velocity, ρ is the density of sea water, C_T is the thrust coefficient, C_D is the drag
 110 coefficient, A_r is the swept area of the rotor and A_s is the frontal area of the support structure. The operation and
 111 output of the turbine is controlled by the pitch of the rotor blades, resulting in changes in the thrust and power
 112 coefficient. The methodology used to represent the operation of the tidal turbines is presented by Plew & Stevens

113 (2013) [24]. Below the cut-in speed the rotor produces no power, meaning the thrust and power coefficient are
 114 zero, i.e. $C_T = C_P = 0$. Between the cut-in speed U_C and the rated speed U_D it is assumed the pitch of the rotor
 115 blade is fixed along with the tip speed ratio, resulting in a constant thrust and power coefficient C_{T0} and C_{P0} .
 116 Above the rated speed the pitch of the rotor blade is increased to reduce the power produced and maintaining rated
 117 power P_D . The power coefficient is parameterised as:

$$118 \quad C_P = \frac{2P_D}{\rho A_r U^3}, \quad U > U_D, \quad (2)$$

119 For simplicity, Plew and Stevens assume a fixed relationship between the thrust and power coefficient, resulting
 120 in the thrust coefficient above rated speed being parameterised as:

$$121 \quad C_T = \frac{C_{T0}}{C_{P0}} \frac{2P_D}{\rho A_r U^3}, \quad U > U_D \quad (3)$$

122 The resolutions of unstructured meshes are typically larger than the modelled turbines, therefore, the drag force
 123 is spread over the area of several elements. An unstructured mesh can result in elements of different sizes, thus a
 124 different force may be applied to different elements within the same area defined as one turbine. Therefore, a
 125 regular mesh using triangular elements is used in the area where turbines are modelled, ensuring any variation is
 126 due to the hydrodynamics and not the mesh. The resolution of these regular meshes is 20m. Each device is
 127 represented individually, with the force of each device spread over eight elements. For Ramsey Sound and Sound
 128 of Islay, the array layout is set as detailed by the site developer. The single turbine within Strangford Loch is
 129 positioned as deployed. For the remaining site, each array is made up of rows that stretch the permissible width
 130 of the site, with a lateral spacing between devices of two and half rotor diameters [25]. For arrays with multiple
 131 rows, the devices are ten rotor diameters downstream of each other [25] in a staggered formation [26].

132 Over the eight tidal developments, five different tidal technologies have been proposed. Ramsey Sound will
 133 use Delta Stream devices; Strangford Loch, Anglesey, West of Islay and Fair Head will use Atlantis Resource's
 134 MCT SeaGen-S; Torr Head will use Openhydro; Sound of Islay will use Hammerfest and Mull of Kintyre will
 135 use Nautricity. For all the projects, each device is modelled individually. Furthermore, each technology type is
 136 parameterised differently in the model. The turbine parameters for each device can be found in Table 1. As the
 137 SeaGen-S, Nautricity and Delta Stream device have multiple rotors, the total force of these devices is combined
 138 into one device. For simplicity, all the support structures have been assumed to be single cylindrical monopiles,
 139 with the exception of Openhydro and Nautricity. Openhydro has two monopoles and Nautricity is a tethered
 140 floating turbine. The drag coefficient for the cylindrical monopile was $C_D=0.9$. The drag of the tether has been
 141 ignored due to its negligible drag force.

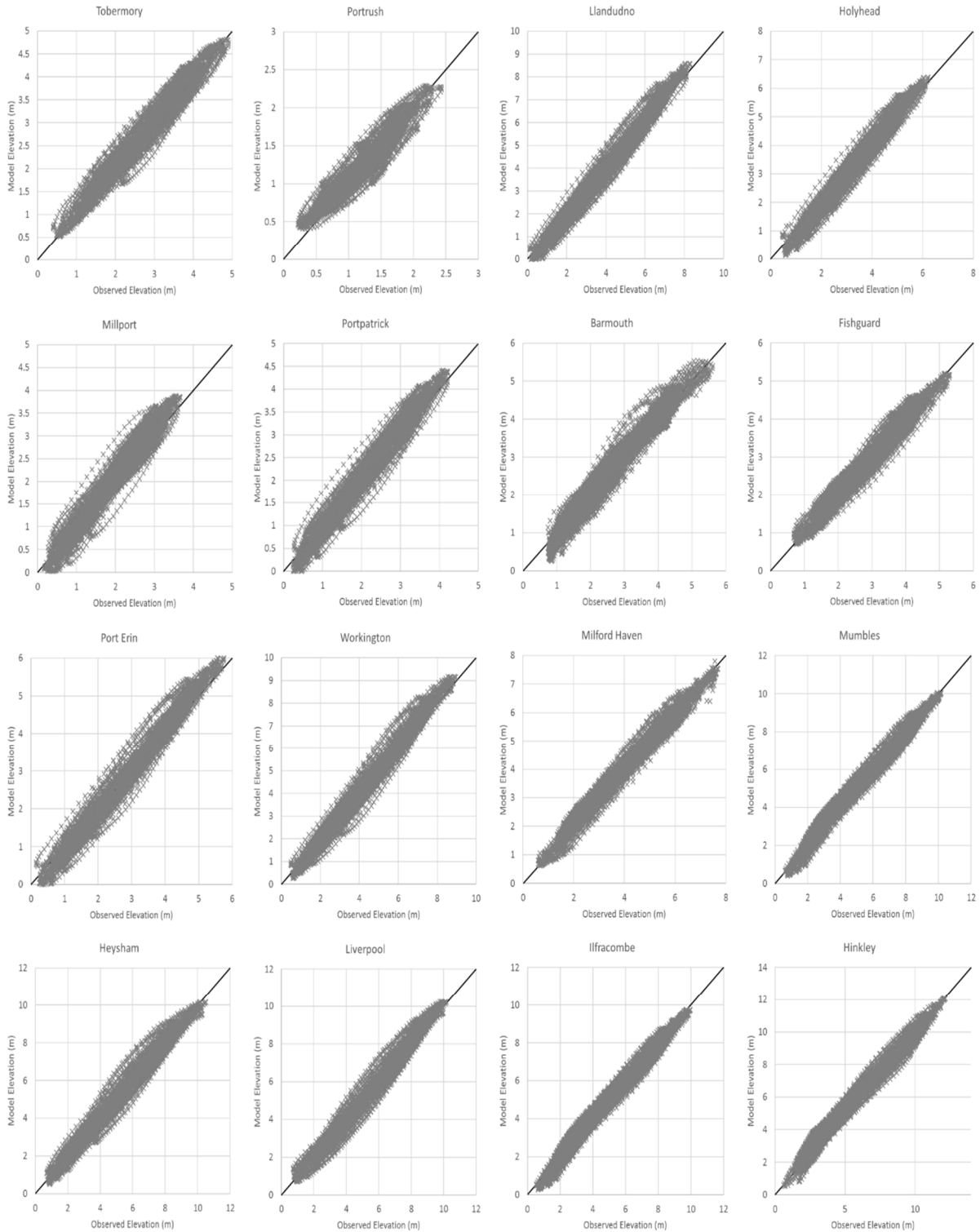
142 **Table 1: Characteristics of the five device technologies used to parameterise the turbines in the model.**

| Device | Rate Power (MW) | Rotor Diameter (m) | Hub Height (m) | Monopile Diameter (m) | U_C (m/s) | U_D (m/s) | C_{T0} | C_{P0} |
|--------------|-----------------------|--------------------------|----------------------|-----------------------------|----------------|----------------|----------|----------|
| Delta stream | 1.2 | 18 | 15 | 2 | 0.8 | 2.25 | 0.81 | 0.27 |
| SeaGen-S | 2 | 20 | 15 | 2 | 0.8 | 2.5 | 0.8 | 0.41 |
| Openhydro | 2 | 16 | 16 | 2 | 0.8 | 3.5 | 0.8 | 0.45 |
| Hammerfest | 1 | 23 | 22 | 2 | 0.8 | 2.5 | 0.7 | 0.33 |
| Nautricity | 0.5 | 14 | 12 | 0 | 0.8 | 2.5 | 0.8 | 0.41 |

143 4 Validation

144 4.1 Free surface elevations

145 Validation data has been obtained from the British Oceanographic Data Centre (BODC) [12] for surface
 146 elevation at sixteen tide gauges, whose locations are shown in Figure 1. After a 5 day spin-up period, the model
 147 was run for 30 days from 17/05/2012 00:00 to 16/06/2012 00:00. Comparisons of the modelled free surface
 148 elevation and observed tidal elevations at each tide gauge are shown in Figure 2.
 149



150

151 **Figure 2: Comparison of observed and modelled free surface elevation. The black line represents a $y=x$ relationship**
 152 **with the dashed line representing a regression line of best fit.**

153 The results in Figure 2 illustrate the validation between modelled and observed values, and show these are in
 154 close agreement at the tide gauges in the southern half of the model (Fishguard, Milford Haven, Mumbles,
 155 Ilfracombe and Hinkley) which includes the Severn Estuary. Tide gauges in the central Irish Sea, such as
 156 Barmouth, Millport, Portpatrick and Port Erin show a larger scattering due to a phase misalignment. This is due
 157 to features, e.g. River Clyde, Afon Mawddach and Lough Foyle, being clipped from the model to improve
 158 computational efficiency. Portrush shows some disagreement, however, this may be more due to errors in the tide
 159 gauge rather than the model, as a number of erroneous records were removed from the tide gauge data.

160 To validate the free surface elevations, three statistical quantities have been used: the coefficient of
 161 determination, the root mean squared error and the scatter index. The coefficient of determination, R², is the
 162 proportion of the variance explained by a linear regression model predicting the dependant variable from the
 163 independent variable as is defined as:

$$164 \quad 1 - \frac{\sum_i (y_i - \bar{y}_i)^2}{\sum_i (\hat{y}_i - \bar{y}_i)^2} \quad (4)$$

165 where y_i are the observed values, \bar{y}_i is the mean of the observed values and \hat{y}_i are the predicted values. The value
 166 of R² ranges between 0 and 1, with 0 representing no correlation between predicted and observed values and 1
 167 representing a perfect correlation. The root mean squared error (RMSE) is the standard deviation of error between
 168 the observed and predicted values and is defined as:

$$169 \quad \sqrt{\frac{1}{n} \sum_{i=1}^n (\hat{y}_i - y_i)^2} \quad (5)$$

170 where n is the total number of observations. The scatter index is RMSE normalised by the mean of the
 171 observations:

$$172 \quad \frac{RMSE}{\bar{y}_i} \times 100\% \quad (6)$$

173 Table 2 summarises the validation statistics of the sixteen tide gauges.

174 **Table 2: Validation statistics of the 16 tide gauges.**

| Tide Gauge | R ² | RMSE (m) | Scatter Index (%) |
|---------------|----------------|-------------|----------------------|
| Tobermory | 0.965 | 0.200 | 7.54 |
| Portrush | 0.901 | 0.149 | 5.64 |
| Millport | 0.950 | 0.260 | 9.83 |
| Portpatrick | 0.969 | 0.235 | 8.88 |
| Port Erin | 0.974 | 0.301 | 11.35 |
| Workington | 0.977 | 0.381 | 14.38 |
| Heysham | 0.974 | 0.407 | 15.36 |
| Liverpool | 0.974 | 0.403 | 15.19 |
| Llandudno | 0.976 | 0.387 | 14.58 |
| Holyhead | 0.968 | 0.308 | 11.63 |
| Barmouth | 0.948 | 0.287 | 10.82 |
| Fishguard | 0.952 | 0.236 | 8.89 |
| Milford Haven | 0.974 | 0.280 | 10.56 |
| Mumbles | 0.978 | 0.368 | 13.87 |
| Illfracombe | 0.977 | 0.363 | 13.67 |
| Hinkley | 0.975 | 0.506 | 19.07 |

175 The coefficient of determination shows that there is a good correlation between the observed and modelled free
 176 surface. However, the RMSE and scatter index indicate a poorer correlation. As the free surface varies about the
 177 mean sea level, the difference between the mean of the observed and the predicted will always be small. The
 178 difference between time series are more likely to be due to uncertainty in the location of the tide gauges than an
 179 error in the model [27].

180 4.2 Harmonic Analysis

181 The model was run for 30 days to provide a time series of sufficient length to permit a harmonic analysis which
 182 includes the dominant components. The dominant components are the M2 and S2 constituents. Table 3 and Table
 183 4 show the comparison between harmonic constituents from the UKHO and the model for the M2 and S2
 184 constituents for tidal elevations. Figure 3 plots the comparison between the modelled and observed M2 & S2
 185 constituent amplitude for tidal elevations.

186 **Table 3: Comparison between observed and modelled M2 constituent for tidal elevations.**

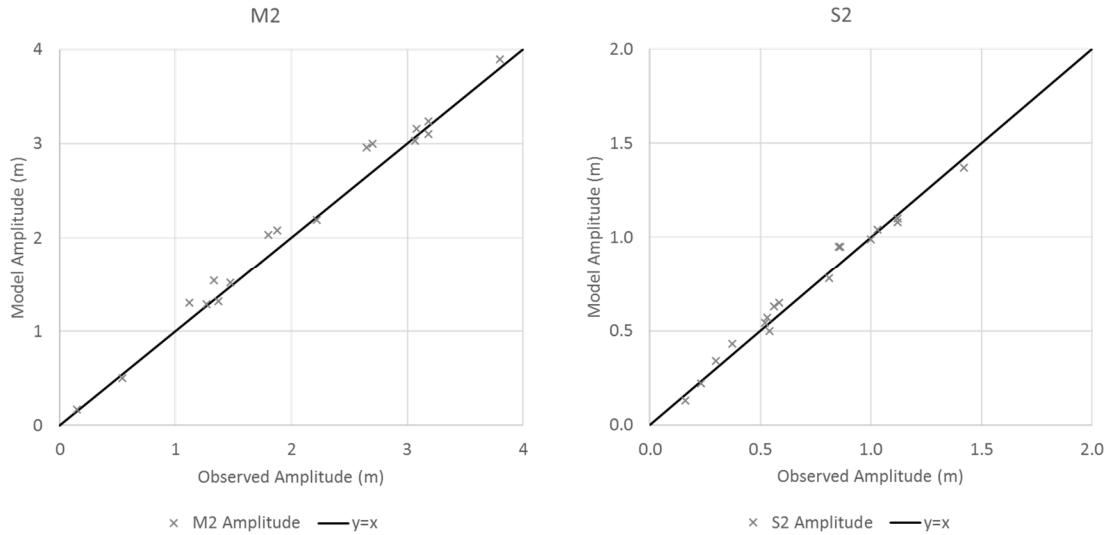
| Tide Gauge | M2 | | | | | |
|---------------|------------------------|---------------------|---------------------------|----------------------|-------------------|---------------------------|
| | Observed Amplitude (m) | Model Amplitude (m) | Percentage Difference (%) | Observed Phase (deg) | Model Phase (deg) | Percentage Difference (%) |
| Tobermory | 1.27 | 1.29 | 1.6 | 175.0 | 168.1 | -1.9 |
| Port Ellen | 0.15 | 0.17 | 13.3 | 50.3 | 52.2 | 0.5 |
| Portrush | 0.54 | 0.50 | -7.4 | 201.0 | 203.9 | 0.8 |
| Millport | 1.12 | 1.30 | 16.1 | 341.0 | 341.3 | 0.1 |
| Portpatrick | 1.33 | 1.54 | 15.8 | 331.0 | 330.8 | -0.1 |
| Port Erin | 1.88 | 2.08 | 10.7 | 322.7 | 321.2 | -0.4 |
| Workington | 2.70 | 3.00 | 11.2 | 333.7 | 330.5 | -0.9 |
| Heysham | 3.18 | 3.24 | 1.9 | 325.0 | 321.7 | -0.9 |
| Liverpool | 3.08 | 3.16 | 2.6 | 315.2 | 318.6 | 1.0 |
| Llandudno | 2.65 | 2.96 | 11.8 | 310.1 | 310.3 | 0.1 |
| Holyhead | 1.80 | 2.03 | 12.8 | 292.0 | 294.3 | 0.6 |
| Barmouth | 1.47 | 1.52 | 3.4 | 244.0 | 241.5 | -0.7 |
| Fishguard | 1.37 | 1.32 | -3.6 | 208.0 | 212.2 | 1.2 |
| Milford Haven | 2.22 | 2.19 | -1.4 | 173.0 | 172.6 | -0.1 |
| Mumbles | 3.18 | 3.10 | -2.5 | 171.0 | 171.6 | 0.2 |
| Ilfracombe | 3.07 | 3.03 | -1.3 | 163.0 | 162.3 | -0.2 |
| Hinkley | 3.80 | 3.90 | 2.6 | 185.0 | 181.5 | -1.0 |

187

188 **Table 4: Comparison between observed and modelled S2 constituents for tidal elevations.**

| Tide Gauge | S2 | | | | | |
|---------------|------------------------|---------------------|---------------------------|----------------------|-------------------|---------------------------|
| | Observed Amplitude (m) | Model Amplitude (m) | Percentage Difference (%) | Observed Phase (deg) | Model Phase (deg) | Percentage Difference (%) |
| Tobermory | 0.52 | 0.54 | 3.8 | 211.0 | 204.4 | -1.8 |
| Port Ellen | 0.16 | 0.13 | -18.8 | 141.0 | 143.9 | 0.8 |
| Portrush | 0.23 | 0.22 | -4.3 | 216.0 | 212.7 | -0.9 |
| Millport | 0.30 | 0.34 | 13.3 | 33.0 | 31.9 | -0.3 |
| Portpatrick | 0.37 | 0.43 | 15.8 | 16.0 | 15.0 | -0.3 |
| Port Erin | 0.56 | 0.63 | 12.3 | 2.9 | 1.3 | -0.4 |
| Workington | 0.86 | 0.95 | 11.0 | 17.3 | 13.6 | -1.0 |
| Heysham | 1.03 | 1.04 | 1.0 | 8.0 | 4.1 | -1.1 |
| Liverpool | 1.00 | 0.99 | -1.0 | 359.2 | 361.7 | 0.7 |
| Llandudno | 0.86 | 0.95 | 10.2 | 352.7 | 351.5 | -0.3 |
| Holyhead | 0.59 | 0.65 | 11.0 | 329.0 | 332.3 | 0.9 |
| Barmouth | 0.53 | 0.57 | 7.5 | 283.0 | 279.8 | -0.9 |
| Fishguard | 0.54 | 0.50 | -7.4 | 249.0 | 253.2 | 1.2 |
| Milford Haven | 0.81 | 0.78 | -3.7 | 218.0 | 217.0 | -0.3 |
| Mumbles | 1.12 | 1.10 | -1.8 | 221.0 | 218.2 | -0.8 |
| Ilfracombe | 1.12 | 1.08 | -3.6 | 209.0 | 208.3 | -0.2 |
| Hinkley | 1.42 | 1.37 | -3.5 | 237.0 | 232.5 | -1.3 |

189



190

191 **Figure 3: Comparison between modelled and observed M2 (left) and S2 (right) tidal constituent for tidal elevations.**

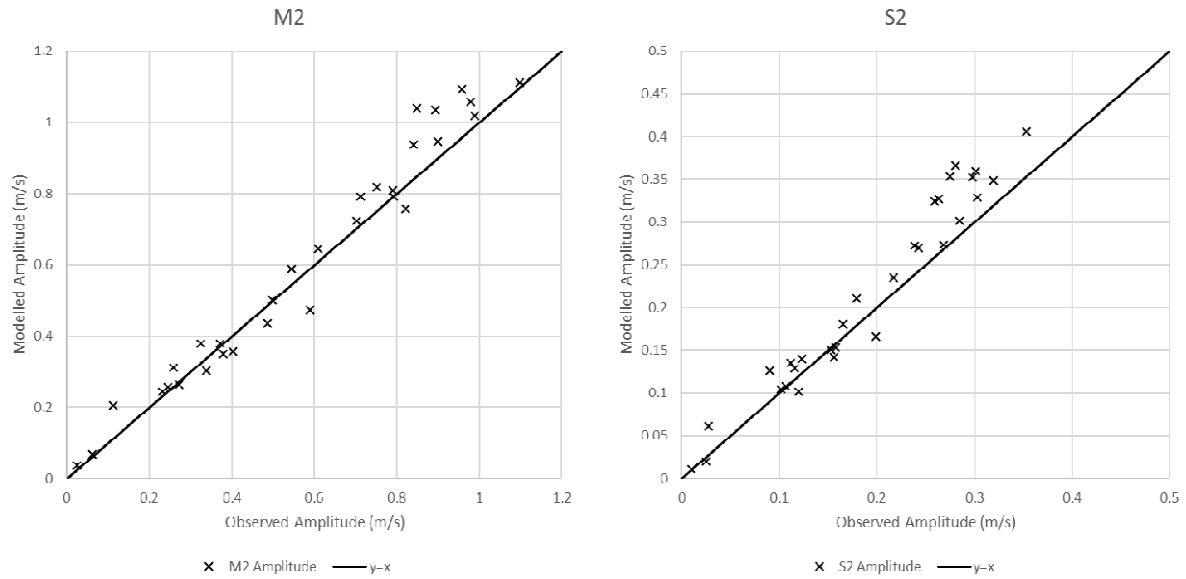
192 Analysis of the harmonics reveals agreement between the model and observations in the northern and southern
 193 parts of the model domain. In the central Irish Sea, the model over-predicts the elevations, on average, by 13%.
 194 Pingree & Griffith (1979) found a similar effect in their model of the Irish Sea [28]. Whilst they found an
 195 improvement by increasing the drag coefficient in this region they could not remove all the discrepancies due to
 196 errors caused by a depth-averaged model. However, the validation of this model is comparable to other studies of
 197 the Irish Sea [13,14]. Table 5 summarises the model validation compared against Robins et al (2015) and Lewis
 198 et al. (2015) with this study. Compared to the tide gauges the scatter index is smaller and within acceptable ranges,
 199 7.44% and 6.93% for the M2 and S2 respectively.

200 **Table 5: Comparison of model validation of tidal elevations with similar studies.**

| RMSE | Present Study | | Robins et al (2015) | | Lewis (2015) | |
|----------------|-------------------|----------------|---------------------|----------------|-------------------|----------------|
| | Amplitude (cm) | Phase (deg) | Amplitude (cm) | Phase (deg) | Amplitude (cm) | Phase (deg) |
| M ₂ | 15 | 3 | 15 | 12 | 13 | 6 |
| S ₂ | 5 | 3 | 5 | 10 | 8 | 14 |

201

202 Along with tidal elevations, a harmonic analysis was performed on the tidal currents. Currents have been
 203 validated against published tidal current ellipse data from 31 offshore current meters (see [11] and [29] for further
 204 details). Figure 4 plots the comparison between the modelled and observed M2 & S2 constituent amplitude for
 205 tidal currents.



206

207

Figure 4: Comparison between modelled and observed M2 (left) and S2 (right) tidal constituent for tidal velocities.

208

209

210

211

212

Analysis of the harmonics reveals agreement between the model and observations. It can be seen that the model does slightly over-estimate the currents, with a bias towards the model of 3.4 cm/s for M2 and 2.4 cm/s for S2. However, the validation of this model is comparable to other studies of the Irish Sea [13,14]. Table 6: Comparison of model validation of tidal currents with similar studies. Table 6 summarises the model validation compared against Robins et al (2015) and Lewis et al. (2015) with this study.

213

Table 6: Comparison of model validation of tidal currents with similar studies.

| RMSE | Present Study Amplitude (cm/s) | Robins et al (2015) Amplitude (cm/s) | Lewis (2015) Amplitude (cm/s) |
|----------------|--------------------------------------|--|-------------------------------------|
| M ₂ | 6.7 | 4.6 | 8 |
| S ₂ | 3.7 | 1.6 | 2 |

214

5 Results – Irish Sea Model

215

216

217

218

219

220

221

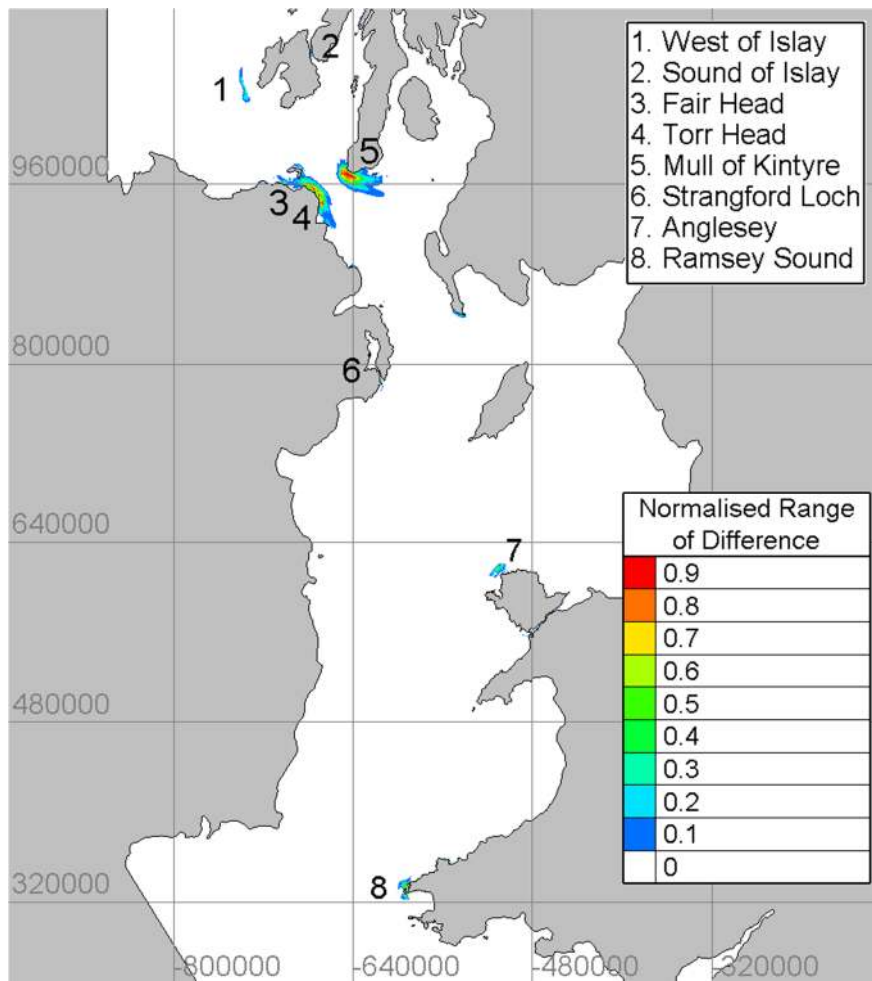
222

223

224

225

To determine if any of the tidal projects were interacting with each other, their zones of influence were calculated using the normalised range of difference. The model is run twice: a base case (without turbines) and a turbine case (with all turbines). The range of difference is calculated by subtracting the magnitude of velocity at each node of the mesh of the turbine run from the magnitude of the velocity in the base case. This is done for each time step, producing a temporally and spatially varying difference between the two models. The range of difference is the difference between the maximum increase and decrease at each node over the whole model run. The range is then normalised to the maximum change to give a percentage figure. The range of difference does not represent the instantaneous velocity reduction due to the direct wake of the turbine array at any one time. Instead, it gives an indication of the total temporal and spatial extent of change. Figure 5 shows the cumulative normalised range of difference for the eight developments over the 30-day model run.



226

227

Figure 5: The cumulative zones of influence for all eight tidal projects, calculated using the range of difference.

228

229

230

231

232

The normalised range of difference from Ramsey Sound (10MW), the Anglesey Skerries (10MW), Strangford Loch (1.2MW), West of Islay (30MW) and the Sound of Islay (10MW) are sufficiently small that their zones of influence do not overlap. However, Fair Head and Torr Head do overlap. The zone of influence for Mull of Kintyre is large given the scale of project (3MW), especially when compared to Fair Head (100MW) and Torr Head (100MW). Fair Head and Torr Head may be influencing the Mull of Kintyre as well.

233

6 Northern Ireland Model

234

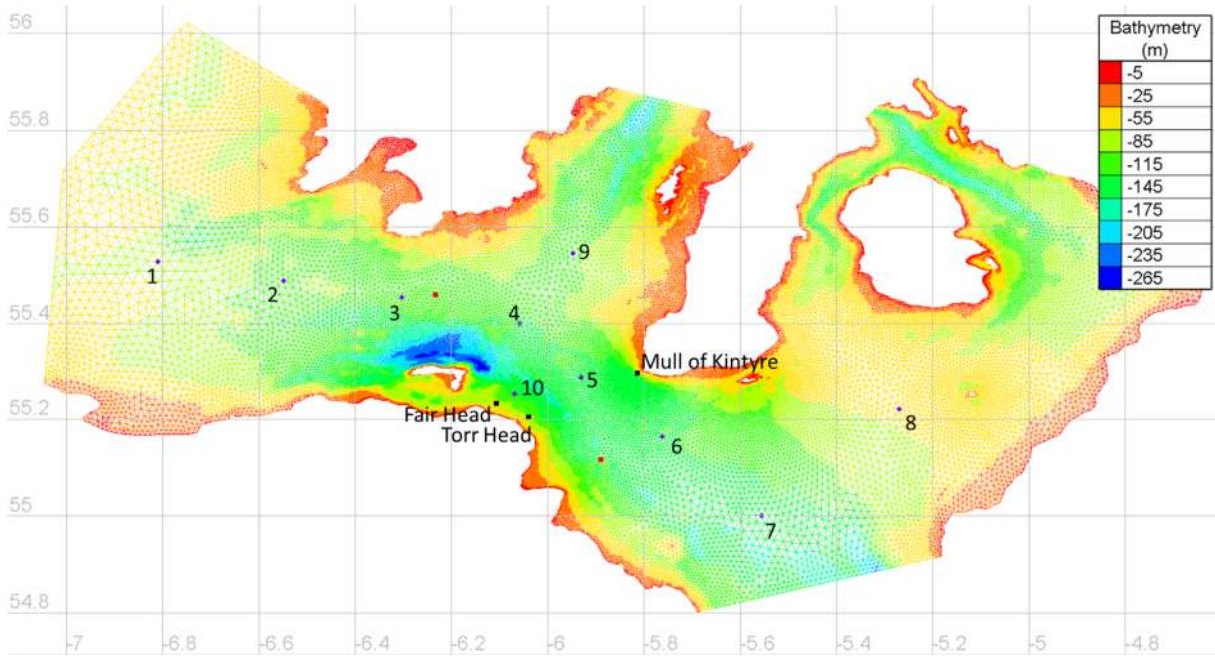
235

236

237

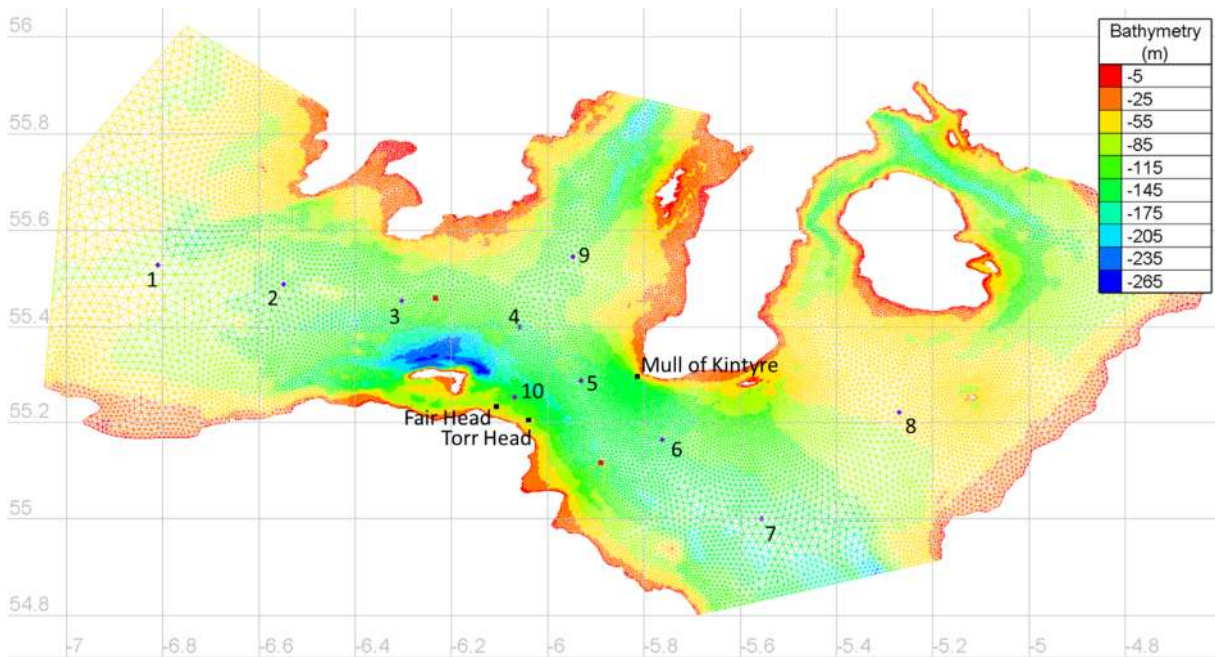
As the model domain is computationally expensive to run, a smaller model domain encompassing these three projects was created to further investigate the interaction. The Northern Ireland model uses the same structure as the full Irish Sea model but only covers the smaller area of interest. It uses the same coastline and bathymetry as the previous model. The model domain extends between 54.80°N – 56.02°N and 4.62°W – 7.04°W and is shown

238 in



239
240
241
242
243

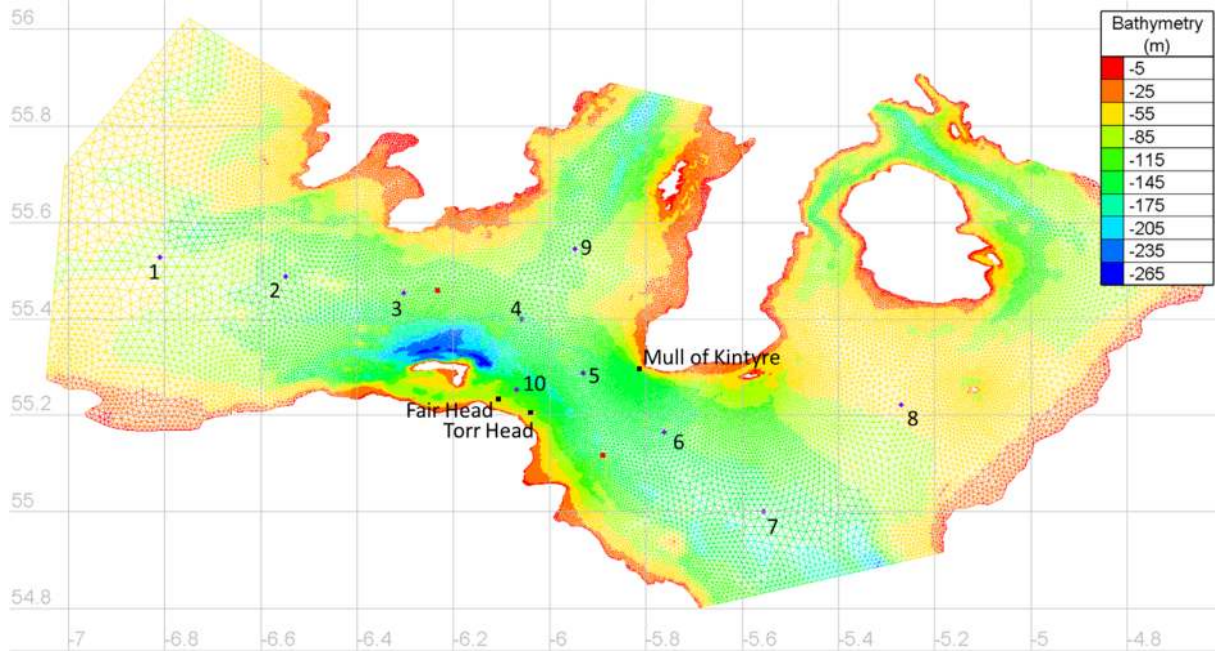
Figure 6. The unstructured mesh was discretised with 137,000 nodes. A regular mesh using triangular elements is used in the area where turbines are modelled. The resolution of the regular mesh is 20m. The model was run over the same period of time as the Irish Sea model.



244
245
246

Figure 6: Northern Ireland model domain. Locations of the tidal arrays are indicated in black dots, the tidal elevation validation points in purple diamonds and current observations in red squares.

247 After a 5-day spin-up period, the model base case was run for 30 days to allow enough time to include a
 248 sufficient number of harmonic components in the analysis. Harmonic constituents at ten locations (see



249

250 Figure 6) were extracted from the TPXO database to validate the model. Table 7 &

| M2 | | | | | | |
|----------|------------------------|---------------------|----------------|----------------------|-------------------|------------------|
| Location | Observed Amplitude (m) | Model Amplitude (m) | Difference (m) | Observed Phase (deg) | Model Phase (deg) | Difference (deg) |
| 1 | 0.64 | 0.61 | -0.03 | 164.2 | 164.0 | -0.1 |
| 2 | 0.40 | 0.36 | -0.04 | 158.1 | 154.9 | -3.2 |
| 3 | 0.13 | 0.08 | -0.06 | 137.9 | 145.4 | 7.5 |
| 4 | 0.11 | 0.18 | 0.07 | 344.9 | 338.3 | -6.6 |
| 5 | 0.38 | 0.41 | 0.03 | 332.3 | 330.2 | -2.2 |
| 6 | 0.74 | 0.72 | -0.02 | 331.7 | 329.0 | -2.7 |
| 7 | 0.98 | 0.99 | 0.01 | 327.8 | 326.5 | -1.2 |
| 8 | 1.02 | 1.03 | 0.01 | 338.9 | 337.6 | -1.3 |
| 9 | 0.18 | 0.22 | 0.04 | 28.5 | 15.0 | -13.6 |
| 10 | 0.33 | 0.36 | 0.02 | 300.8 | 301.7 | 0.9 |

251 Table 8 show the comparison between harmonic constituents from the TPXO database and the model for the
 252 M2 and S2 constituents. Figure 7 shows the comparison between the modelled and observed M2 and S2
 253 constituent amplitude.

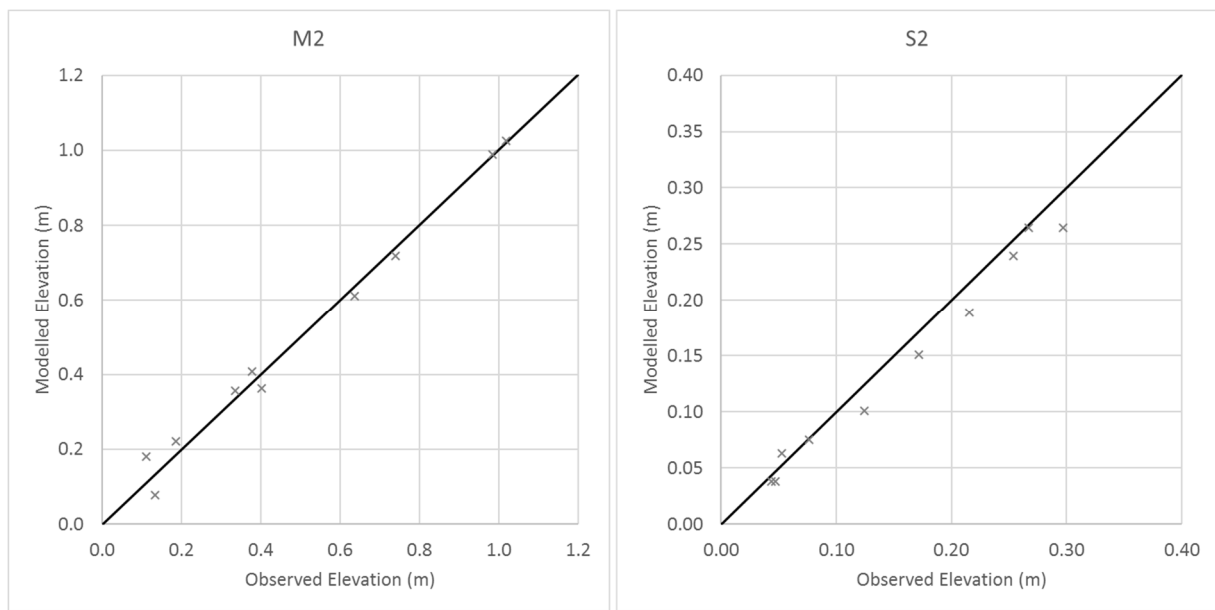
254 **Table 7: Comparison between observed and modelled M2 constituent.**

| M2 | | | | | | |
|----------|------------------------|---------------------|----------------|----------------------|-------------------|------------------|
| Location | Observed Amplitude (m) | Model Amplitude (m) | Difference (m) | Observed Phase (deg) | Model Phase (deg) | Difference (deg) |
| 1 | 0.64 | 0.61 | -0.03 | 164.2 | 164.0 | -0.1 |
| 2 | 0.40 | 0.36 | -0.04 | 158.1 | 154.9 | -3.2 |
| 3 | 0.13 | 0.08 | -0.06 | 137.9 | 145.4 | 7.5 |
| 4 | 0.11 | 0.18 | 0.07 | 344.9 | 338.3 | -6.6 |
| 5 | 0.38 | 0.41 | 0.03 | 332.3 | 330.2 | -2.2 |
| 6 | 0.74 | 0.72 | -0.02 | 331.7 | 329.0 | -2.7 |
| 7 | 0.98 | 0.99 | 0.01 | 327.8 | 326.5 | -1.2 |
| 8 | 1.02 | 1.03 | 0.01 | 338.9 | 337.6 | -1.3 |
| 9 | 0.18 | 0.22 | 0.04 | 28.5 | 15.0 | -13.6 |
| 10 | 0.33 | 0.36 | 0.02 | 300.8 | 301.7 | 0.9 |

255 **Table 8: Comparison between observed and modelled S2 constituent.**

| Location | S2 | | | | | |
|----------|------------------------|---------------------|----------------|----------------------|-------------------|------------------|
| | Observed Amplitude (m) | Model Amplitude (m) | Difference (m) | Observed Phase (deg) | Model Phase (deg) | Difference (deg) |
| 1 | 0.30 | 0.26 | -0.03 | 194.9 | 194.4 | -0.5 |
| 2 | 0.22 | 0.19 | -0.03 | 189.3 | 185.0 | -4.3 |
| 3 | 0.12 | 0.10 | -0.02 | 178.2 | 176.5 | -1.7 |
| 4 | 0.05 | 0.04 | -0.01 | 161.0 | 133.1 | -27.8 |
| 5 | 0.05 | 0.06 | 0.01 | 28.4 | 29.9 | 1.6 |
| 6 | 0.17 | 0.15 | -0.02 | 15.5 | 16.6 | 1.1 |
| 7 | 0.25 | 0.24 | -0.01 | 9.4 | 10.3 | 0.9 |
| 8 | 0.27 | 0.26 | 0.00 | 22.2 | 24.1 | 1.9 |
| 9 | 0.08 | 0.08 | 0.00 | 136.3 | 121.4 | -14.9 |
| 10 | 0.04 | 0.04 | -0.01 | 306.4 | 314.4 | 8.0 |

256

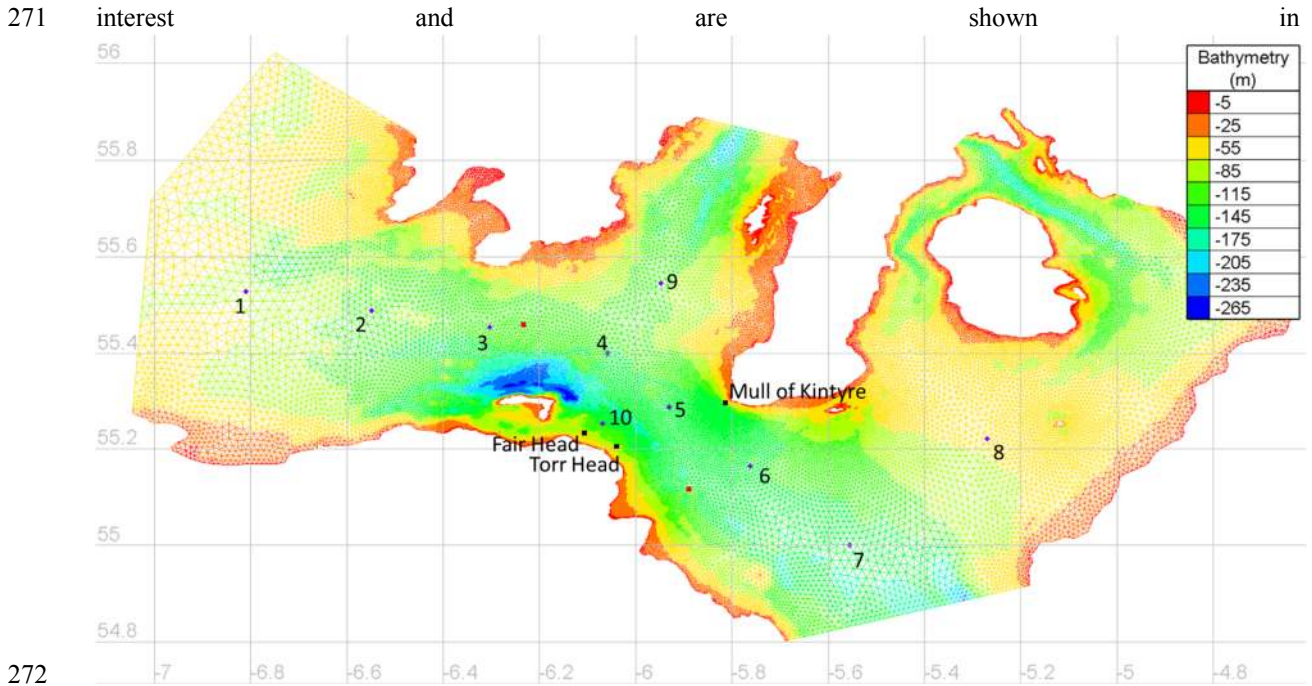


257

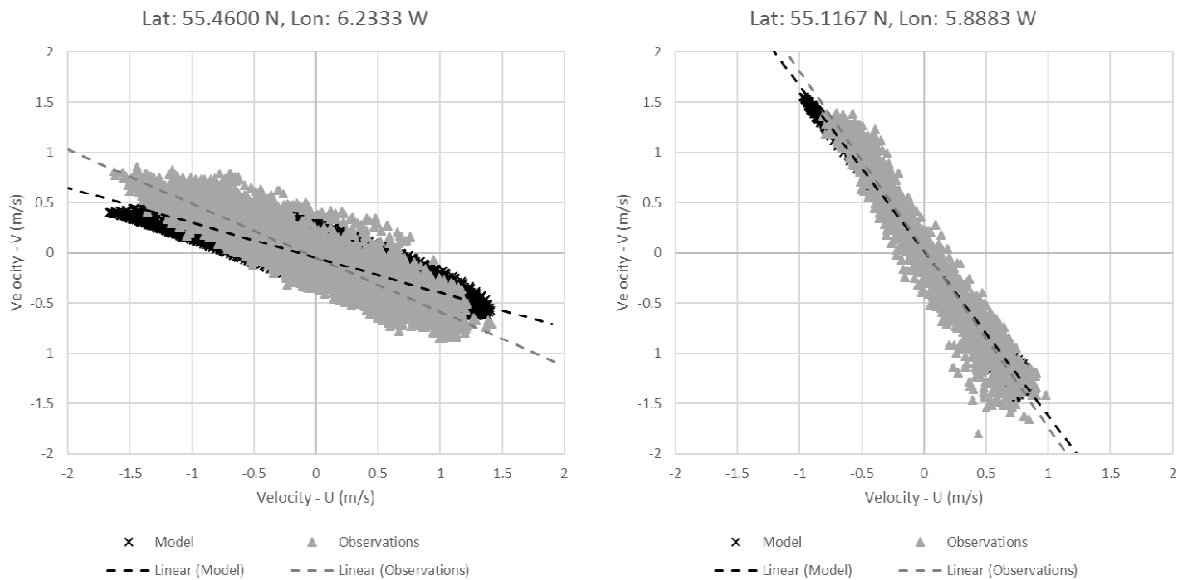
258 **Figure 7: Comparison between modelled and observed M2 (left) and S2 (right) tidal constituent.**

259 Results show the Northern Ireland model validates better than the Irish Sea domain. The RMSE of the M2 and
 260 S2 amplitude is 4cm and 2cm, respectively, with a scatter index of 7.55% and 3.62%. However, this may be due
 261 to the model being validated using harmonics from the same database that drives the model. As the Irish Sea
 262 model was validated against tide gauge data, the harmonics from the Northern Ireland model were also compared
 263 against the harmonics of the Irish Sea model at the ten locations. The M2 amplitude of the Northern Ireland model
 264 is on average 4cm smaller than the Irish Sea model. The S2 amplitude is on average 2cm smaller. The Irish Sea
 265 model was found to be slightly over predicting the amplitude of the M2 and S2 constituent, meaning that the
 266 smaller amplitudes in the Northern Ireland model show an improvement. As the model shows close agreement to
 267 both the TPXO database and the Irish Sea model, the validation of Northern Ireland model will be considered
 268 adequate for this study.

269 As insufficient points from the previous harmonic analysis lie within the smaller model domain, current
 270 observations were obtained from the BODC [12]. The two validation points lie to the east and west of the sites of



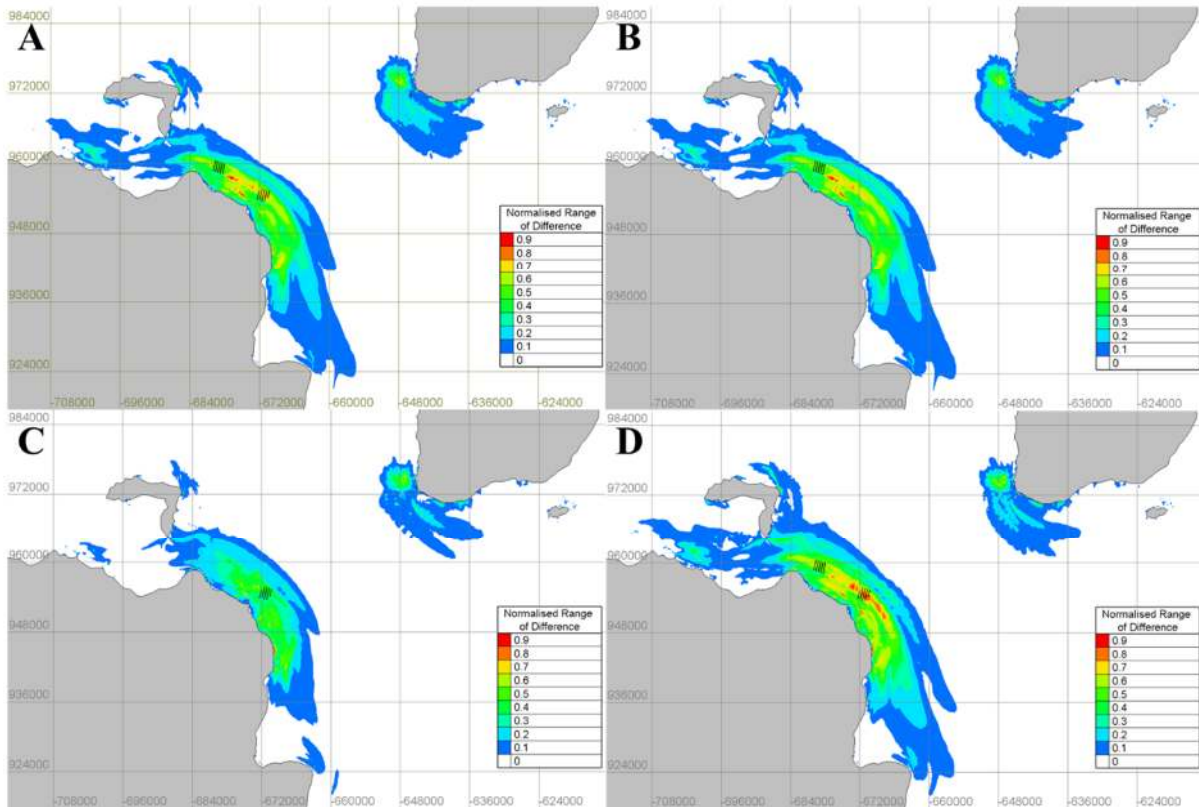
273 Figure 6. The first observation point was located at 55.46°N and 6.2333°W and recorded tidal velocities
 274 between 13-09-1994 16:25 and 29-10-1994 08:35, with a ten-minute interval. The second observation point was
 275 located 55.1167°N and 5.8883°W and recorded tidal velocities between 08-05-1995 12:15 and 08-06-1995 08:35,
 276 with a ten-minute interval. As the period of observation does not match the period of the model, a direct
 277 comparison cannot be made. However, it can be seen in Figure 8, that both the shape and magnitude of the tidal
 278 velocities are in good agreement.



280 **Figure 8: Comparison between modelled and observed tidal velocities at 55.46°N, 6.2333°W and 55.1167°N, 5.8883°W.**

281 **7 Results – Northern Ireland model**

282 The base case was run for 30 days to allow for a harmonic analysis for validating the model. The model runs
 283 containing the tidal turbines were limited to the first 10 days, after the 5-day spin-up. This period encompasses
 284 the peak spring tidal velocities. Figure 9 shows the zone of influence for case 8 (all three projects within the
 285 Northern Ireland model), case 2 (only Fair Head), case 3 (only Torr Head), and case 5 (Fair Head and Torr Head).



286

287 **Figure 9: Cumulative zone of influence for A) case 8 (all three projects), B) case 2 (only Fair Head), C) case 3 (only**
 288 **Torr Head) and D) case 5 (Fair Head and Torr Head).**

289 In Figure 9-a, the zone of influence around Fair Head and Torr Head extends to a range of approximately 75km.
 290 In comparison, the zone of influence around Mull of Kintyre is approximately 20km. This is larger than expected
 291 given Mull of Kintyre is using relatively small 500kW devices. The presence of Fair Head and Torr Head systems
 292 running together lead to impact off the Mull of Kintyre coastline, regardless of the presence of the 3MW tidal
 293 development, as seen in Figure 9-b, c & d. Results indicate that Fair Head is having a larger impact than Torr
 294 Head and the spatial extent of change due to Fair Head alone is similar to the spatial extent where all three projects
 295 are modelled together. The true influence of Fair Head can be seen more clearly from the energy production. Table
 296 9 shows the energy produced over the 10-day period. Table 10 shows the percentage difference in energy
 297 production.

298 **Table 9: Energy production of each tidal project for all eight test cases.**

| Case | Fair Head (MWh) | Torr Head (MWh) | Mull of Kintyre (MWh) |
|------|-----------------|-----------------|-----------------------|
| 1 | - | - | - |
| 2 | 4942.0 | - | - |
| 3 | - | 4179.4 | - |
| 4 | - | - | 423.2 |
| 5 | 4828.6 | 3470.9 | - |
| 6 | 4934.7 | - | 423.6 |
| 7 | - | 4155.4 | 423.4 |
| 8 | 4817.1 | 3464.8 | 423.6 |

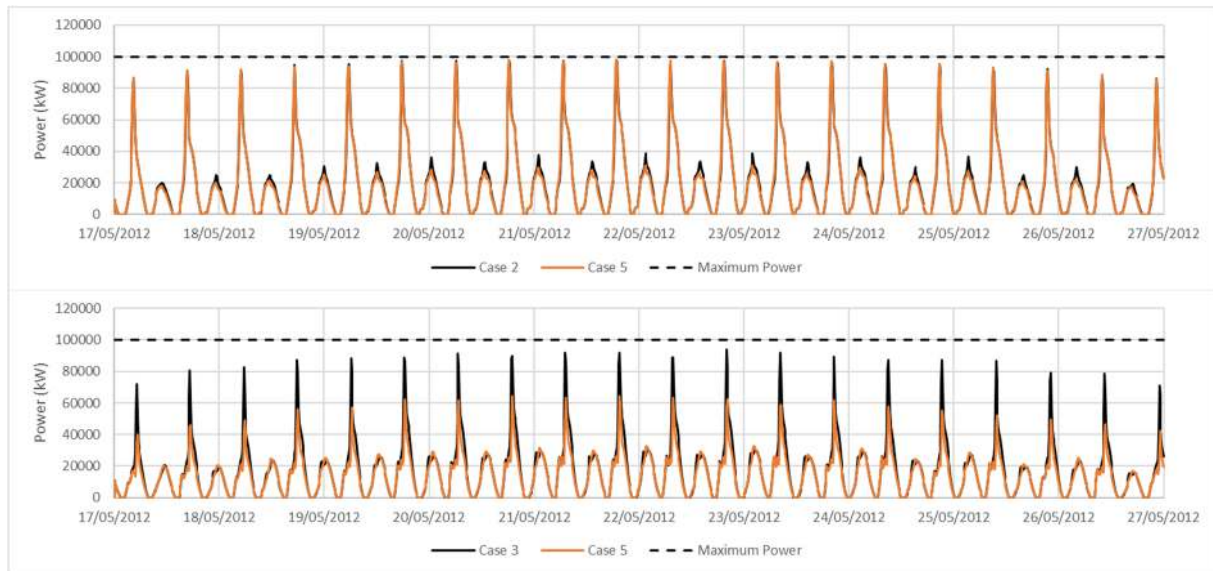
299 **Table 10: Percentage change in energy production for cases 5 – 8.**

| Case | % Difference | | |
|------|--------------|-----------|-----------------|
| | Fair Head | Torr Head | Mull of Kintyre |
| 5 | -2.29 | -16.95 | - |
| 6 | -0.15 | - | 0.09 |
| 7 | - | -0.57 | 0.05 |
| 8 | -2.53 | -17.10 | 0.09 |

300 From the energy production it can be seen that the interaction between Mull of Kintyre and the other projects
 301 is an order of magnitude smaller than the interaction between Fair Head and Torr Head. The Mull of Kintyre
 302 project benefits in all cases with the inclusion of Fair Head and Torr Head. Torr Head loses the most energy in
 303 this study. The total energy production at Fair Head is reduced by over 2% due to Torr Head, whereas, Torr Head
 304 itself loses 17% due to the presence of Fair Head.

305 **8 Discussion**

306 The difference in energy production between Fair Head and Torr Head is caused by a large tidal asymmetry
 307 between the flood and the ebb tide. The flood (west to east) is considerably stronger than the ebb (east to west)
 308 and can clearly be seen in the power production. Figure 10 shows the total instantaneous power production for
 309 Fair Head and Torr Head for cases 2, 3 and 5 (both arrays operating separately and operating concurrently).



310 **Figure 10: Total power production for Fair Head (top) and Torr Head (bottom). The solid black line represents the**
 311 **power production from each array separately (case 2 & 3) and the solid orange represents both Fair Head and Torr**
 312 **Head operating concurrently (case 5). The dash black line represents the maximum total power output of each array**
 313

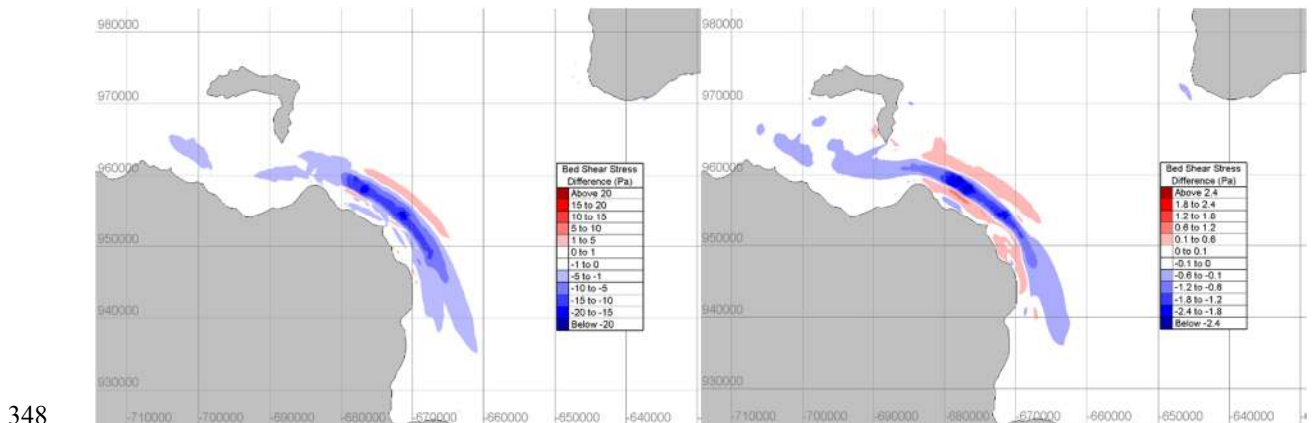
314 When both arrays operate separately, the power production is approximately 4-5 times larger on the flood tide
 315 than the ebb tide. As Fair Head is situated to the west of Torr Head, the tidal asymmetry means that Fair Head has
 316 a larger detrimental effect on Torr Head. During the flood tide, Fair Head extracts energy from the flow reducing
 317 the peak velocities at Torr Head such that the power production at Torr Head is reduced to approximately two
 318 thirds the power output as if it was operating in isolation. Whereas, during an ebb tide when the flow is slower,
 319 the presence of Torr Head only reduces the power output at Fair Head by 20%. Despite both arrays having an
 320 installed capacity of 100 MW, when operated in isolation, Fair Head never exceeds 40 MW on the ebb and Torr
 321 Head never exceeds 30 MW. Furthermore, due to the intra-array effects, the total maximum power output is 97.8
 322 MW for Fair Head and 93.8MW for Torr Head, when operated separately. When the two sites are operated
 323 concurrently, the maximum power during the flood tide is 98.1MW for Fair Head and 64.5 MW for Torr Head.
 324 This represents a 31% reduction in peak power output. This is considerably more than when considering the
 325 reduction in tidal resource from wave-current interactions. The inclusion of waves can reduce the tidal resource
 326 by 20% in extreme conditions and by 15% in winter mean conditions [17]. The proximity and position of the two
 327 tidal sites mean they will share similar wave resources, meaning a reduction in resource will affect both sites. By
 328 reducing tidal currents, the impact of Fair Head would reduce during the flood, increasing the power output at

329 Torr Head. However, extreme conditions only affect a small portion of the year, meaning the impact on the annual
 330 energy production is still present. Further work would be required to quantify the effect wave-current interaction
 331 at this study location.

332 Maximising the power output within in the constraint of the Levelised Cost of Energy of a tidal project is
 333 considered best single outcome for optimising the cumulative deployment of tidal stream energy extraction [4].
 334 But, it should also be considered in partnership with the constraint of minimising the environmental impact. The
 335 economic viability of tidal energy is not considered within this study. It is clear that with a 17% reduction in
 336 energy production, if deployed alongside Fair Head, Torr Head would lose a considerable amount of revenue.
 337 However, if Torr Head could still operate commercially despite the presence of Fair Head then there are
 338 environmental positives. Comparing the zones of influence in Figure 9 the spatial extent of change is similar. If
 339 Fair Head is built, then the additional impact of Torr Head is reduced. Other impacts should also be considered.
 340 Hydrodynamics are a primary driver in physical processes, such as suspended sediments, sediment transport and
 341 substrate composition. A more accurate predictor of the impact on physical processes would be the changes to
 342 mean and maximum bed shear stress as this can give a perspective of change over a longer timescale. Bed shear
 343 stress is calculated as:

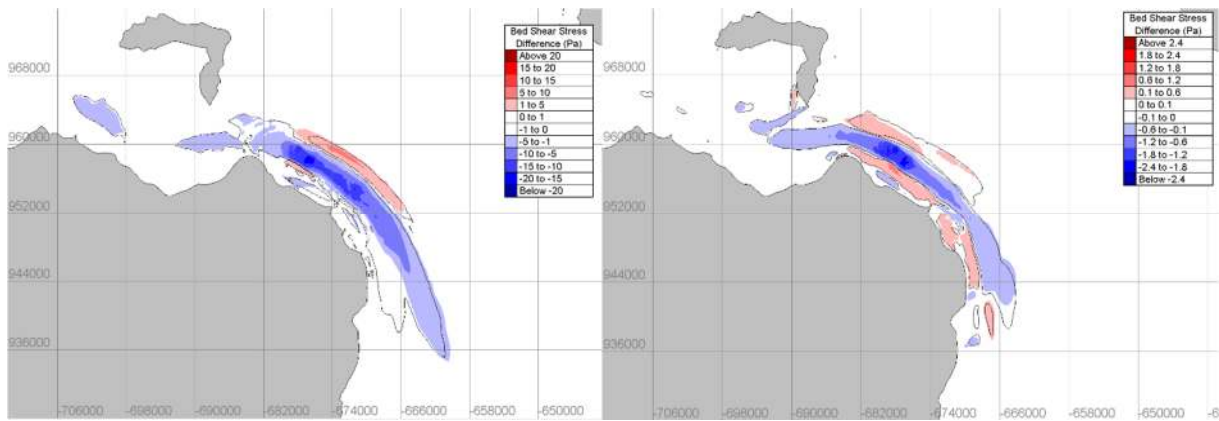
$$344 \quad \tau = \rho C_d \|\mathbf{u}\| \mathbf{u}. \quad (7)$$

345 where ρ is the density of seawater, C_d is the bottom drag coefficient and $\|\mathbf{u}\|$ is the magnitude of the velocity
 346 vector. For the purpose of calculating bed shear stress, the value $C_d = 0.0025$ was used. Figure 11 shows the
 347 maximum and mean change in bed shear stress for case 8 (all three projects).



348
 349 **Figure 11: Variation in maximum bed shear stress (left) and mean bed shear stress (right).**

350 Case 8 represents the worst case scenario with all three projects present. Whilst a change could be seen around
 351 the Mull of Kintyre in Figure 9, the impact on the mean and maximum bed shear stress is minimal. The major
 352 change is limited to the vicinity of Fair Head and Torr Head. For case 8, the peak reduction in maximum bed shear
 353 stress is 23.2 Pa. The peak reduction in mean bed shear stress is 2.6 Pa. These values are similar to changes seen
 354 in the Pentland Firth, as modelled in [5]. When only Fair Head is present the peak reduction in maximum and
 355 mean bed shear stress is 17.5 Pa and 2.4 Pa respectively. Figure 12 show the maximum and mean change in bed
 356 shear stress for case 2. The black contour represents the extent of change for case 8, as shown in Figure 11.



357

358 **Figure 12: Variation in maximum bed shear stress (left) and mean bed shear stress (right) for case 2. The black contour**
 359 **represents the spatial extent of change for case 8.**

360 The spatial extent between case 2 and case 8 is very similar. In both cases sediment would accumulate within
 361 the vicinity of the arrays with areas of erosion either side. The turbines are located in areas that are void of any
 362 fine sediment and are mainly gravel or exposed bed rock [19]. The magnitude of change would result in medium
 363 gravel accumulating in an area of coarse gravel so the impact is likely to be minimal. This change would occur
 364 within the Torr Head site with or without the presence of Torr Head if Fair Head was present. Sand is present
 365 between the coastline and the tidal turbines and the resulting increase in bed shear stress would likely cause erosion
 366 in this area. However, the magnitude of bed shear stress increase is similar in both case 2 and 8. The maximum
 367 increase in bed shear stress for case 8 is 4.5 Pa. For case 2 it is 4.0 Pa. The mean increase in both cases is 0.7 Pa.
 368 Whilst the seabed around Fair Head and Torr Head is mainly gravel, 40 km to the west is the Skerries and
 369 Causeway Special Area of Conservation (SAC). One of the primary designations of the SAC was the protection
 370 of sandbanks. It has been shown that tidal stream devices can influence the maintenance of sandbanks [23]. In this
 371 case study, the effect should be minimal. The net transport of sediment to the SAC is from the west [28] and the
 372 large tidal asymmetry means any accumulation within the vicinity of the tidal array should transport eastwards.
 373 However, the only way to be certain is to use the methodology shown in [16], which can determine the array size
 374 that would not cause an impact above natural variation is sediment transport.

375 There is a clear interaction between Fair Head and Torr Head. This is due to their proximity and installed
 376 capacity. Likewise, with the lack of interaction with the other six sites. The installed capacity of the other sites is
 377 significantly smaller than Fair Head and Torr Head. Thus, their zone of influence is much smaller. Although, not
 378 investigated, the interaction between Ramsey Sound, Anglesey and Fair/Torr Head, would likely be minimal if
 379 their rated capacity were all equal. This is due to distances between the sites. It is approximately 175km between
 380 Ramsey Sound and Anglesey and 225km between Anglesey and Fair/Torr Head. The risk of interaction to these
 381 sites will be when more intermediary sites are developed. The risk of interaction between other forms of energy
 382 extraction in the Irish Sea, i.e. offshore wind and tidal barrages, will be of little risk. The reduction in tidal
 383 velocities due to wind turbine monopile structures is negligible [31]. There is no interaction between tidal stream
 384 devices and tidal barrages in the Irish Sea [4]. Whilst the deployment of tidal stream extraction remains small,
 385 ~10MW, the risk of interaction within the Irish Sea is small. As the industry grows and the technology matures,
 386 allowing sites with lower peak velocities to be exploited, the risk of interaction will grow. Other tidal sites, such
 387 as in the Pentland Firth, where there are four proposed projects geographically within 20km of each other, the
 388 potential for interaction is significantly higher.

389 9 Conclusions

390 A cumulative impact assessment of eight tidal stream developments, totaling 264 MW, in the Irish Sea has been
 391 undertaken using a high-resolution depth-averaged hydrodynamic model. Results show that five of the eight tidal
 392 projects run quite independently of each other. However, projects at Fair Head, Torr Head and Mull of Kintyre
 393 lie within each other's zone of influence. Due to the computational expense of running the model, a second smaller
 394 model was developed which included only these three projects.

395 Results of the second model show that the Mull of Kintyre project had very little impact on the energy
 396 production at Fair Head and Torr Head. Energy production slightly increased (+0.09%) at the Mull of Kintyre
 397 with the presence of the other two projects. For the two remaining projects, Fair Head had a greater impact on
 398 Torr Head than the other way. Torr Head reduces energy production at Fair Head by 2%, whereas Fair Head
 399 reduces energy production by 17% at Torr Head. On closer examination, this is due to the tidal asymmetry at the

400 site. The flood (west-east) is stronger than the ebb. As Fair Head lies to the west of Torr Head, the impact is
401 greater. Despite both arrays having an installed capacity of 100 MW, the maximum power during the flood tide
402 is 98.1MW for Fair Head and 64.5 MW for Torr Head. Due to the intra-array effects, the total maximum power
403 output is 97.8 MW for Fair Head and 93.8MW for Torr Head, when operated separately. This represents a 31%
404 reduction in peak power output at Torr Head.

405 Whilst the economics may allow Fair Head to operate commercially with a slight reduction in energy
406 production, a further detailed analysis would be required to determine if Torr Head remains economically viable.
407 However, if Torr Head can still operate commercially in the presence of Fair Head, then the additional
408 environmental impact of Torr Head, such as the change in bed shear stress, is small.

409 Within the Irish Sea, very few tidal projects investigated are geographically within close proximity of each
410 other, meaning their interaction is limited. Whilst the deployment of tidal stream extraction remains small,
411 ~10MW, the risk of interaction within the Irish Sea is small. As the industry grows and the technology matures,
412 allowing sites with lower peak velocities to be exploited, the risk of interaction to these sites will grow when more
413 intermediary sites are developed.

414 **10 Acknowledgment**

415 The Industrial Doctorate Centre for Offshore Renewable Energy is funded by the Energy Technologies Institute
416 and the RCUK Energy Programme, grant number (EP/J500847/1). This work was carried out on the High
417 Performance Computing Cluster supported by the Research and Specialist Computing Support service at the
418 University of East Anglia.

419 **References**

- 420 [1] Neill, S.P., Vögler, A., Goward-Brown, A.J., Baston, S., Lewis, M.J., Gillibrand, P.A., Waldman, S. and Woolf, D.K.
421 (2017) The wave and tidal resource of Scotland. *Renewable Energy*: in press. Available online 16 March 2017.
- 422 [2] RenewableUK (2015) Wave and Tidal Energy in the UK – Capitalising on Capability, [Online], Available:
423 <http://www.renewableuk.com/en/publications/index.cfm/>.
- 424 [3] Fairley, I., Masters, I. and Karunaratna, H. (2015) The cumulative impact of tidal stream turbine arrays on sediment
425 transport in the Pentland Firth. *Renewable Energy*, 80, pp.755-769.
- 426 [4] Wilson, S., Bourban, S. and Couch, S. (2012). Understanding the interactions of tidal power projects across the UK
427 continental shelf. In 4th International Conference on Ocean Energy, Dublin.
- 428 [5] Martin-Short, R., Hill, J., Kramer, S.C., Avdis, A., Allison, P.A. and Piggott, M.D. (2015) Tidal resource extraction in the
429 Pentland Firth, UK: Potential impacts on flow regime and sediment transport in the Inner Sound of Stroma. *Renewable Energy*,
430 76, pp.596-607.
- 431 [6] Draper, S., Adcock, T.A., Borthwick, A.G. and Houlby, G.T. (2014). Estimate of the tidal stream power resource of the
432 Pentland Firth. *Renewable Energy*, 63, pp.650-657.
- 433 [7] Woolf, D.K. (2013) The strength and phase of the tidal stream. *Int. J. Marine Energy*, 3, p.4.
- 434 [8] Robinson, I.S. (1979) The tidal dynamics of the Irish and Celtic Seas. *Geophysical Journal International*, 56(1), pp.159-
435 197.
- 436 [9] Pingree, R.D. and Griffiths, D.K. (1987) Tidal friction for semidiurnal tides. *Continental shelf research*, 7(10), pp.1181-
437 1209.
- 438 [10] Davies, A.M. and Jones, J.E. (1992). A three dimensional model of the M2, S2, N2, K1 and O1 tides in the Celtic and
439 Irish Seas. *Progress in Oceanography*, 29(3), pp.197-234.
- 440 [11] Young, E.F., Aldridge, J.N. and Brown, J. (2000) Development and validation of a three-dimensional curvilinear model
441 for the study of fluxes through the North Channel of the Irish Sea. *Continental Shelf Research*, 20(9), pp.997-1035.
- 442 [12] British Oceanographic Data Centre, Tidal observations, [Online], Available: <http://www.bodc.ac.uk/>.
- 443 [13] Robins, P.E., Neill, S.P., Lewis, M.J. and Ward, S.L. (2015) Characterising the spatial and temporal variability of the
444 tidal-stream energy resource over the northwest European shelf seas. *Applied Energy*, 147, pp.510-522.
- 445 [14] Lewis, M., Neill, S.P., Robins, P.E. and Hashemi, M.R. (2015). Resource assessment for future generations of tidal-stream
446 energy arrays. *Energy*, 83, pp.403-415.
- 447 [15] Neill, S.P., Hashemi, M.R. and Lewis, M.J. (2014) Optimal phasing of the European tidal stream resource using the
448 greedy algorithm with penalty function. *Energy*, 73, pp.997-1006.
- 449 [16] Robins, P.E., Neill, S.P. and Lewis, M.J. (2014) Impact of tidal-stream arrays in relation to the natural variability of
450 sedimentary processes. *Renewable Energy*, 72, pp.311-321.
- 451 [17] Hashemi, M.R., Neill, S.P., Robins, P.E., Davies, A.G. and Lewis, M.J. (2015) Effect of waves on the tidal energy resource
452 at a planned tidal stream array. *Renewable Energy*, 75, pp.626-639.
- 453 [18] Walkington, I. and Burrows, R. (2009) Modelling tidal stream power potential. *Applied Ocean Research*, 31(4), pp.239-
454 245.
- 455 [19] Telemac, [Online], Available: <http://www.opentelemac.org/>.
- 456 [20] OSU Tidal Data Inversion, [Online], Available: <http://volkov.oce.orst.edu/tides/>.

- 457 [21] Rastogi, A.K. and Rodi, W. (1978) Predictions of heat and mass transfer in open channels. *Journal of the Hydraulics*
458 *division*, 104(3), pp.397-420.
- 459 [22] Ahmadian, R., Falconer, R. and Bockelmann-Evans, B. (2012) Far-field modelling of the hydro-environmental impact of
460 tidal stream turbines. *Renewable Energy*, 38(1), pp.107-116.
- 461 [23] Neill, S.P., Jordan, J.R. and Couch, S.J. (2012) Impact of tidal energy converter (TEC) arrays on the dynamics of headland
462 sand banks. *Renewable Energy*, 37(1), pp.387-397.
- 463 [24] Plew, D.R. and Stevens, C.L. (2013) Numerical modelling of the effect of turbines on currents in a tidal channel – Tory
464 Channel, New Zealand, *Renewable Energy*, 57, p269-282.
- 465 [25] EMEC (2009) Assessment of Tidal Energy Resource, [Online], Available: [http://www.emec.org.uk/assessment-of-tidal-](http://www.emec.org.uk/assessment-of-tidal-energy-resource/)
466 [energy-resource/](http://www.emec.org.uk/assessment-of-tidal-energy-resource/).
- 467 [26] Couch, S.J. and Bryden, I.G. (2007) Large-scale physical response of the tidal system to energy extraction and its
468 significance for informing environmental and ecological impact assessment. In: *Proceedings Oceans 2007-Europe*
469 *International Conference 2007*, pp. 912–916.
- 470 [27] Gunn, K. and Stock-Williams, C. (2013). On validating numerical hydrodynamic models of complex tidal flow.
471 *International Journal of Marine Energy*, 3, pp.e82-e97.
- 472 [28] Pingree, R.D. and Griffiths, D.K. (1979). Sand transport paths around the British Isles resulting from M 2 and M 4 tidal
473 interactions. *Journal of the Marine Biological Association of the United Kingdom*, 59(02), pp.497-513.
- 474 [29] Jones, J.E. (1983) Charts of the O1, K1, N2, M2 and S2 tides in the Celtic Sea including M2 and S2 tidal currents. Institute
475 of Oceanographic Sciences, Report No.169.
- 476 [30] Tidal Ventures (2015) Torr Head Tidal Energy Array EIA, [Online], Available:
477 http://www.tidalventures.com/downloads/environmentalstatement/ES_9_Benthic&IntertidalEcology.pdf.
- 478 [31] Zhang W., Xia H., Wang B. (2009) Numerical Calculation of the Impact of Offshore Wind Power Stations on
479 Hydrodynamic Conditions. In: *Advances in Water Resources and Hydraulic Engineering*. Springer, Berlin, Heidelberg.